# Mapping the gravitational wave background

Neil J. Cornish§

Department of Physics, Montana State University, Bozeman, MT 59717, USA

Abstract. The gravitational wave sky is expected to have isolated bright sources superimposed on a diffuse gravitational wave background. The background radiation has two components: a confusion limited background from unresolved astrophysical sources; and a cosmological component formed during the birth of the universe. A map of the gravitational wave background can be made by sweeping a gravitational wave detector across the sky. The detector output is a complicated convolution of the sky luminosity distribution, the detector response function and the scan pattern. Here we study the general de-convolution problem, and show how LIGO (Laser Interferometric Gravitational Observatory) and LISA (Laser Interferometer Space Antenna) can be used to detect anisotropies in the gravitational wave background.

### 1. Introduction

Gravitational wave detectors are fairly blunt instruments. In the low frequency limit, which corresponding to wavelengths large compared to the effective size of the detector, a gravitational wave detector's antenna pattern has only monopole, quadrupole and sextupole components. Despite this limitation, it is in principle possible to locate a source with arbitrary precision so long as the signal-to-noise ratio is large and the motion of the detector with respect to the source is sufficiently fast and varied.

Gravitational wave detectors get their directional information from the amplitude and frequency modulation that occur as the antenna pattern is swept across the sky. The frequency modulation is due to the Doppler shift caused by the relative motion of the source and the detector. For example, orbital motion about the Sun creates a periodic frequency shift with amplitude  $\delta f/f \sim 10^{-4} \sin \theta$ , where  $\theta$  is the co-latitude in ecliptic coordinates. The amplitude modulation occurs as the antenna lobes are swept across the sky. For the LIGO detectors[1] this occurs with a fundamental period of one sidereal day, while for the LISA detector[2] the fundamental period is one sidereal year. When we are lucky enough to have two detectors, differences in the arrival time can be used to furnish further directional information. A discussion of the angular resolution of LIGO can be found in the work of Jaranowski & Królak[3]. Discussions of the angular resolution of LISA can be found in the work of Peterseim et al. [4], Cutler[5] and Hellings & Moore[6].

In addition to individual bright sources of gravitational waves, there will also be a variety of unresolved gravitational wave backgrounds. It is likely that one component of the background will have a cosmological origin - the cosmic gravitational wave background (CGB). However, the dominant contribution is expected to be a confusion background formed by the superposition of many weak point sources, such as white dwarf binaries. The gravitational wave backgrounds will be approximately stochastic, making them difficult to distinguish from noise in the detectors. One way around this problem is to cross-correlate the output from two detectors. Since the noise in each detector is uncorrelated while the signal is correlated, the signal-to-noise improves as the square root of the observation time. Typically, this type of correlation has to be done over a finite frequency interval  $\Delta f$  that is large compared to the Doppler modulation  $\delta f$ , so the frequency modulation is washed out. Thus, maps of the gravitational wave background have to be made using amplitude modulation alone.

Here we describe how gravitational wave detectors can be used to create maps of the gravitational wave background. The pioneering work of Allen and Ottewill[7] showed how anisotropies in the gravitational wave background will modulate the output from the cross-correlated LIGO detectors. A similar calculation was carried out by Giampieri and Polnorev[8] in the low frequency limit (f < 1 mHz) for the LISA detector. They showed how the signal would be modulated by the antenna's orbital motion. Neither group addressed the inverse problem - that is, how to create a map of the gravitational wave sky from the modulated output. We address the inverse problem and find that

the ground-based detectors that are currently under construction have the ability to produce maps with a resolution of  $\ell \sim 20$  at f=100 Hz, where  $\ell$  is the multipole number. This is comparable to the maps of the cosmic microwave background (CMB) produced by the COBE (COsmic Background Explorer) satellite. We find that a single LISA detector can produce a partial map with a resolution of  $\ell \sim 6$  at f=10 mHz, improving to  $\ell \sim 25$  at f=100 mHz. More than one LISA detector needs to be flown to produce a complete map. For example, two LISA detectors with a relative orbital inclination of  $\sim 20$  degrees could produce a complete map with a resolution of  $\ell \sim 8$ .

A full implementation of the theoretical scheme developed here will be published elsewhere[9]. It involves an end-to-end simulation of the data analysis, starting with a synthetic gravitational wave sky that produces a modulated signal from a simulated gravitational wave detector. The detector model incorporates a basic treatment of the anticipated noise. Finally, the simulated signal is deconvolved to produce a sky map that is compared to the original.

### 2. The general convolution problem

Suppose the gravitational wave background has a luminosity distribution given by  $\mathcal{L}(\theta, \phi, f)$ . Here  $(\theta, \phi)$  are coordinates on the sky in the CMB rest frame and f is the gravitational wave frequency. The response of a gravitational wave detector can be characterized by a detector response function  $\mathcal{F}(\theta, \phi, f, t)$ . The response varies with time as the detector moves relative to the sky. The detector output C(t, f) is given by the all-sky integral

$$C(t,f) = \oint_{S^2} \mathcal{L}(\theta,\phi,f) \mathcal{F}(\theta,\phi,f,t) \sin \theta d\theta d\phi.$$
 (1)

Given the time series C(t, f) we need to find the luminosity distribution  $\mathcal{L}(\theta, \phi, f)$ .

It is natural to decompose the luminosity distribution and the detector response function into spherical harmonics in their respective rest frames. Writing  $\vec{e}_{\alpha}$  for basis vectors in the sky frame and  $\vec{e}_{\bar{\alpha}}$  for the detector frame we have

$$\vec{e}_{\alpha} = \Lambda^{\bar{\beta}}_{\alpha}(t) \, \vec{e}_{\bar{\beta}} \quad \Rightarrow \quad \Lambda_{\alpha\bar{\beta}}(t) = \vec{e}_{\alpha} \cdot \vec{e}_{\bar{\beta}} \,,$$
 (2)

where  $\Lambda_{\alpha\bar{\beta}}(t)$  are the components of the coordinate transformation relating the two frames. In practice the gravitational fields will be weak and the velocities slow, so the coordinate transformation is well approximated by a spatial rotation. The coordinates  $(\theta, \phi)$  in the sky frame are related to the coordinates  $(\bar{\theta}, \bar{\phi})$  in the detector frame by

$$\cos \bar{\theta} = \hat{\Omega} \cdot \vec{e}_{\bar{z}} = \sin \theta \cos \phi \, \Lambda_{x\bar{z}} + \sin \theta \sin \phi \, \Lambda_{y\bar{z}} + \cos \theta \, \Lambda_{z\bar{z}} \,, \tag{3}$$

and

$$\sin \bar{\theta} \, e^{i\bar{\phi}} = \hat{\Omega} \cdot (\vec{e}_{\bar{x}} + i\vec{e}_{\bar{y}})$$

$$= \sin \theta \cos \phi (\Lambda_{x\bar{x}} + i\Lambda_{x\bar{y}}) + \sin \theta \sin \phi (\Lambda_{y\bar{x}} + i\Lambda_{y\bar{y}}) + \cos \theta (\Lambda_{z\bar{x}} + i\Lambda_{z\bar{y}})$$
(4)

We have written the transformations in this form since these are the combinations that appear in the spherical harmonics:

$$Y_{\ell m}(\theta, \phi) = \sqrt{\frac{2\ell + 1}{4\pi} \frac{(\ell - m)!}{(\ell + m)!}} \left( -\sin\theta \, e^{i\phi} \right)^m \frac{d^m}{d(\cos\theta)^m} P_{\ell}(\cos\theta) \,. \tag{5}$$

Decomposing  $\mathcal{L}(\theta, \phi, f)$  and  $\mathcal{F}(\theta, \phi, f, t)$  in the sky frame we have

$$\mathcal{L}(\theta, \phi, f) = \sum_{\ell m} p_{\ell m}(f) Y_{\ell m}(\theta, \phi), \quad \text{and} \quad \mathcal{F}(\theta, \phi, f, t) = \sum_{\ell m} a_{\ell m}(f, t) Y_{\ell m}(\theta, \phi), \tag{6}$$

while in the detector's restframe we have

$$\mathcal{F}(\bar{\theta}, \bar{\phi}, f) = \sum_{\ell m} \bar{a}_{\ell m}(f) Y_{\ell m}(\bar{\theta}, \bar{\phi}). \tag{7}$$

The multipole moments in the two frames are related by

$$a_{\ell m}(f,t) = \sum_{n=-\ell}^{\ell} \bar{a}_{\ell n}(f) \lambda_{\ell m n}(t), \qquad (8)$$

where

$$\lambda_{\ell mn}(t) = \oint_{S^2} Y_{\ell m}^*(\theta, \phi) Y_{\ell n}(\bar{\theta}, \bar{\phi}) d\Omega.$$
 (9)

Using equations (3), (4) and (5) it is a simple matter to calculate the transformation coefficients  $\lambda_{\ell mn}(t)$ . From the properties of the spherical harmonics it follows that

$$\lambda_{\ell mn}^* = (-1)^{m+n} \lambda_{\ell - m - n} \,. \tag{10}$$

Thus, there we only need to calculate  $(2\ell+1)(\ell+1)$  components at order  $\ell$ . Out to order  $\ell=1$  we have

$$\lambda_{000}(t) = 1$$

$$\lambda_{1-10}(t) = \frac{1}{\sqrt{2}} \left( \Lambda_{xz}(t) + i\Lambda_{yz}(t) \right)$$

$$\lambda_{1-11}(t) = \frac{1}{2} \left( -\Lambda_{xx}(t) + \Lambda_{yy}(t) - i\Lambda_{xy}(t) - i\Lambda_{yx}(t) \right)$$

$$\lambda_{100}(t) = \Lambda_{zz}(t)$$

$$\lambda_{110}(t) = \frac{1}{\sqrt{2}} \left( -\Lambda_{xz}(t) + i\Lambda_{yz}(t) \right)$$

$$\lambda_{101}(t) = -\frac{1}{\sqrt{2}} \left( \Lambda_{zx}(t) + i\Lambda_{zy}(t) \right)$$

$$\lambda_{111}(t) = \frac{1}{2} \left( \Lambda_{xx}(t) + \Lambda_{yy}(t) + i\Lambda_{xy}(t) - i\Lambda_{yx}(t) \right) . \tag{11}$$

Higher orders in  $\ell$  involve higher powers of  $\Lambda_{ij}(t)$ . For example,

$$\lambda_{210}(t) = \frac{\sqrt{6}}{2} \Lambda_{zz}(t) \left( -\Lambda_{xz}(t) + i\Lambda_{yz}(t) \right) . \tag{12}$$

Using the decompositions defined in (6), we can express the detector output in terms of the multipole moments  $p_{\ell m}(f)$  and  $a_{\ell m}(t)$ :

$$C(t,f) = \sum_{\ell,m} (-1)^m p_{\ell m}(f) a_{\ell - m}(t,f).$$
(13)

In most instances the detector scan pattern will be periodic in time, so it is natural to Fourier transform all time dependent quantities:

$$A_k = \frac{1}{2\pi} \int_0^{2\pi} d\alpha \, e^{-ik\alpha} A(\alpha) \,, \tag{14}$$

where  $\alpha = 2\pi t/T_0$ , and  $T_0$  is the period of the detector sweep. We can write

$$C_k(f) = \sum_{\ell,m} p_{\ell m}(f) \gamma_{k\ell m}(f) \tag{15}$$

where

$$\gamma_{k\ell m}(f) = (-1)^m a_{k\ell - m}(f) = (-1)^m \sum_{n = -\ell}^{\ell} \bar{a}_{\ell n}(f) \, \lambda_{k\ell - mn} \,. \tag{16}$$

It is a simple matter to calculate the  $\gamma_{k\ell m}$  if we know the detector response function  $\mathcal{F}$  and the scan pattern  $\Lambda_{ij}(t)$ . The de-convolution problem comes down to solving the linear system of equations

$$C_k(f) = p_i(f) \gamma_{ki}(f) \text{ where } i = \ell^2 + \ell + m + 1.$$
 (17)

The  $\gamma_{ki}(f)$  are known, the  $C_k(f)$  are measured experimentally, and the  $p_i(f)$  are what we want to find. Typically the system of equations will be both under and over constrained, but a best fit solution can be found by way of a singular value decomposition.

# 3. Map making with LIGO

We begin by studying how LIGO can be used to map the gravitational wave sky as a prelude to studying the space-based LISA detector. Allen and Ottewill[7] showed how the cross-correlated response of the Hanford and Livingston LIGO detectors is modulated as the rotation of the Earth sweeps the antenna pattern across the sky. However, they stopped short of solving the deconvolution problem to make a map of the gravitational wave sky.

In a sky-fixed reference frame the response of a single LIGO detector to a plane gravitational wave  $\mathbf{h}(t, \mathbf{x}, f)$  with frequency f, propagating in the  $\widehat{\Omega}$  direction is given by

$$s(t) = \mathbf{D}(t) : \mathbf{h}(t, \mathbf{x}), \tag{18}$$

where

$$\mathbf{D}(t) = \frac{1}{2} \left( \mathbf{u}(t) \otimes \mathbf{u}(t) - \mathbf{v}(t) \otimes \mathbf{v}(t) \right)$$
(19)

is the detector tensor and  $\mathbf{u}(t)$  and  $\mathbf{v}(t)$  are unit vectors in the direction of the interferometer arms. The response to a general gravitational wave  $\mathbf{h}(t, \mathbf{x})$  can be derived from (18) by first decomposing the wave into a collection of plane waves:

$$\mathbf{h}(t,\mathbf{x}) = \sum_{A=+,\times} \int_{-\infty}^{\infty} df \int_{S^2} d\widehat{\Omega} \ \tilde{h}_A(f,\widehat{\Omega}) e^{-2\pi i f t} e^{2\pi i f \widehat{\Omega} \cdot \mathbf{x}/c} \mathbf{e}^A(\widehat{\Omega}) . \tag{20}$$

Here  $e^+$  and  $e^\times$  are a set of polarization tensors. The signal we wish to analyze is formed by cross-correlating the output of the two LIGO detectors over an integration time T, centered at time t:

$$S(t) = \int_{t-T/2}^{t+T/2} dt' \int_{t-T/2}^{t+T/2} dt'' s_1(t') s_2(t'') Q(t'-t'').$$
 (21)

Here  $s_1(t)$  and  $s_2(t)$  are the outputs of the two detectors and Q is some filter function. A stochastic background of gravitational waves can be characterized by the statistical character of the Fourier amplitudes  $\tilde{h}_A(f, \hat{\Omega})$ . Following Allen and Ottewill we assume that the background can be approximated as a stationary, Gaussian random distribution characterized by the expectation values

$$\langle \tilde{h}_A(f,\widehat{\Omega}) \rangle = 0$$

$$\langle \tilde{h}_A^*(f,\widehat{\Omega})\tilde{h}_{A'}(f',\widehat{\Omega}') \rangle = \frac{1}{2}\delta(f - f')\frac{\delta^2(\widehat{\Omega},\widehat{\Omega}')}{4\pi}\delta_{AA'}S_h(f)P(\widehat{\Omega}), \qquad (22)$$

where  $S_h(f)$  is the power spectral density and  $P(\widehat{\Omega})$  describes the angular distribution. From these relations it follows that the expectation value of S(t) is given by

$$C(t) = \langle S(t) \rangle = \frac{T}{5} \int_{-\infty}^{\infty} df \, S_h(f) \gamma(f, t) \widetilde{Q}(f) \,, \tag{23}$$

where

$$\gamma(f,t) = \frac{5}{8\pi} \int d\widehat{\Omega} P(\widehat{\Omega}) \sum_{A=+,\times} F_1^A(\widehat{\Omega},t) F_2^A(\widehat{\Omega},t) e^{-2\pi i f \widehat{\Omega} \cdot \Delta \mathbf{x}(t)/c} . \tag{24}$$

Here  $\Delta \mathbf{x}(t)$  is a vector connecting the Hanford and Livingston sites and

$$F_i^A(\widehat{\Omega}, t) = \mathbf{D}_i(t) : \mathbf{e}^A. \tag{25}$$

Using  $S_h(f) = S_h(-f)$ ,  $\tilde{Q}(f) = \tilde{Q}^*(-f)$  and  $\gamma(f,t) = \gamma^*(-f,t)$ , we can write the signal as

$$C(t) = \frac{2T}{5} \int_0^\infty df \, S_h(f) \left( \gamma_R(f, t) \widetilde{Q}_R(f) - \gamma_I(f, t) \widetilde{Q}_I(f) \right),, \tag{26}$$

where  $\gamma_R(f,t)$  denotes the real part of  $\gamma(f,t)$  etc.. In contrast to Allen and Ottewill, who considered the broad-band response, we are interested in making narrow band measurements over a small frequency interval of width  $\Delta f$  centered at frequency f. This allows us to make maps of the gravitational wave sky at particular frequencies. To this end we use the top-hat filter

$$\widetilde{Q}(f') = \begin{cases}
q_R + i q_I & f - \frac{\Delta f}{2} \le f' \le f + \frac{\Delta f}{2} \\
q_R - i q_I & -f - \frac{\Delta f}{2} \le f' \le -f + \frac{\Delta f}{2} \\
0 & \text{otherwise}
\end{cases}$$
(27)

so that

$$Q(t) = 2\frac{\sin(\pi t \Delta f)}{\pi t} \left( q_R \cos(2\pi f t) + q_I \sin(2\pi f t) \right). \tag{28}$$

In the time domain the filter decays rapidly for times  $t > 1/\Delta f$ . In choosing  $\Delta f$  we have to ensure that  $1/\Delta f \ll T$ , otherwise the angular variation will be smeared out.

So long as  $\Delta f$  is small compared to the range over which  $S_h(f)$  and  $\gamma(f,t)$  vary, the narrow band response is given by

$$C(t,f) = \frac{2T\Delta f}{5} S_h(f) \left( q_R \gamma_R(f,t) - q_I \gamma_I(f,t) \right). \tag{29}$$

This equation is of the form

$$C(t,f) = \oint_{S^2} \mathcal{L}(\theta,\phi,f) \mathcal{F}(\theta,\phi,f,t) \sin \theta d\theta d\phi, \qquad (30)$$

where the luminosity equals

$$\mathcal{L}(\theta, \phi, f) = S_h(f)P(\widehat{\Omega}), \qquad (31)$$

and the detector response function is given by

$$\mathcal{F}(\theta, \phi, f, t) = \frac{T\Delta f q_R}{4\pi} \sum_{A=+,\times} F_1^A(\widehat{\Omega}, t) F_2^A(\widehat{\Omega}, t) \cos\left(2\pi f \widehat{\Omega} \cdot \Delta \mathbf{x}(t)/c\right)$$

$$+ \frac{T\Delta f q_I}{4\pi} \sum_{A=+,\times} F_1^A(\widehat{\Omega}, t) F_2^A(\widehat{\Omega}, t) \sin\left(2\pi f \widehat{\Omega} \cdot \Delta \mathbf{x}(t)/c\right)$$
(32)

The choice of integration period T results from a trade-off between maximizing the signal (T large) and maximizing the angular resolution (T small). Setting a maximum angular resolution of  $k_{\text{max}}$  fixes the integration period to be (Nyquist's theorem)

$$T = \frac{T_0}{2k_{\text{max}}}. (33)$$

It turns out that there is little to be gained by setting  $k_{\rm max}$  much larger than 50, so we will take  $k_{\rm max}=50$  and set T=861.64 s. Similar considerations apply to the choice of  $\Delta f$ , which for LIGO we will take to be in the range  $\Delta f=1 \to 10$  Hz. A plot of the antenna pattern for the cross-correlated pair of LIGO detectors is shown in Figure 1 for a range of frequencies. As expected, the antenna pattern has more structure at high frequencies.

Now that we have the LIGO signal expressed in terms of the general convolution problem of the last section, it is a simple matter to carry through the analysis. We begin by setting  $\alpha = 2\pi t/T_d$  where  $T_d = 86164$  s is one sidereal day. Choosing Sky-fixed and Earth-fixed coordinate systems with their z axes aligned with the Earth's rotation axis, we find the two frames are related:

$$\vec{e}_{\bar{x}} = \cos \alpha \, \vec{e}_x + \sin \alpha \, \vec{e}_y$$

$$\vec{e}_{\bar{y}} = -\sin \alpha \, \vec{e}_x + \cos \alpha \, \vec{e}_y$$

$$\vec{e}_{\bar{z}} = \vec{e}_z \,, \tag{34}$$

where the bar denotes the Earth-fixed frame. From these relations it follows that

$$\lambda_{k\ell mn} = \delta_{mn} \, \delta_{km},\tag{35}$$

and

$$\gamma_{klm}(f) = \delta_{km}(-1)^m \bar{a}_{\ell-m}(f) = \delta_{km} \gamma_{\ell m}(f). \tag{36}$$

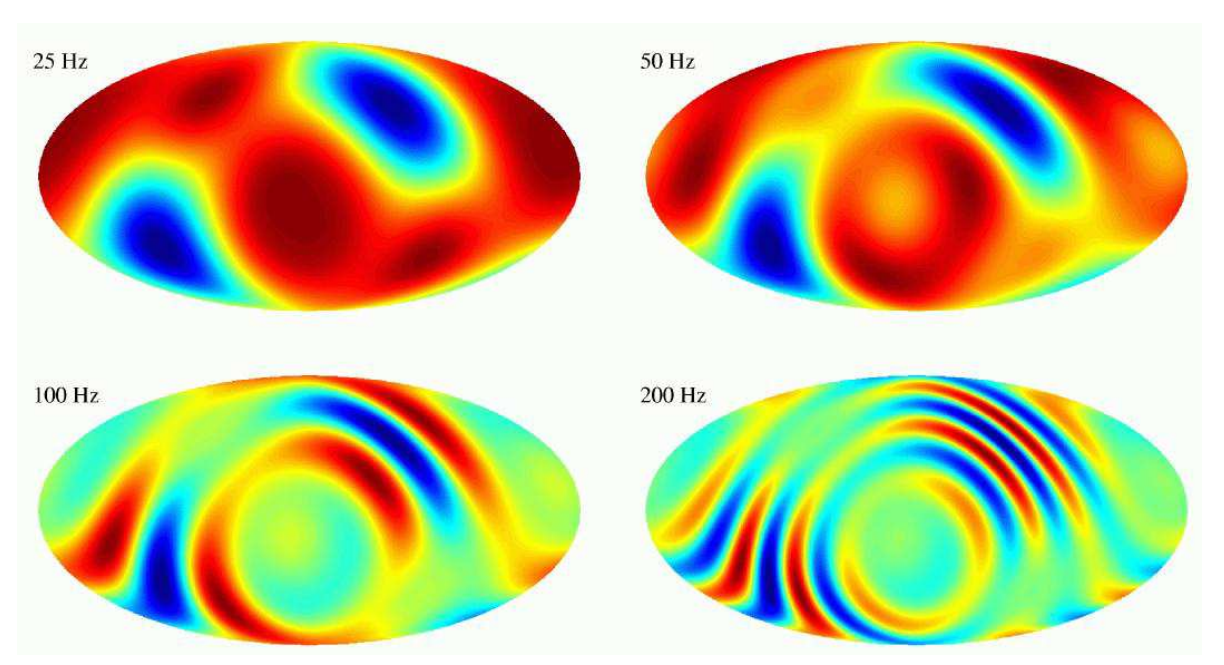


**Figure 1.** The antenna pattern for the cross-correlated LIGO detectors in the Earth-fixed frame,  $\mathcal{F}(\bar{\theta}, \bar{\phi}, f)$ , with  $g_I = 0$  and f = 25, 50, 100 and 200 Hz.

Here  $\gamma_{\ell m}(f)$  correspond to the quantities calculated by Allen and Ottewill. However, they evaluated  $\gamma_{\ell m}(f)$  in an Earth-fixed frame with the z axis parallel to the vector connecting the two detectors,  $\Delta \mathbf{x}$ . A static rotation has to be applied to their results before we can use them. Once this is done we can attack the inversion problem

$$C_k(f) = \sum_{\ell m} p_{\ell m}(f) \gamma_{k\ell m}(f) = \sum_{\ell = |k|}^{\infty} p_{\ell k}(f) \gamma_{\ell k}(f), \qquad (37)$$

where the final line was obtained from the identity

$$\sum_{\ell m} = \sum_{\ell=0}^{\infty} \sum_{m=-\ell}^{\ell} = \sum_{m=-\infty}^{\infty} \sum_{\ell=|m|}^{\infty} . \tag{38}$$

At first sight it appears that we have no hope of solving the inversion problem since it involves  $2(2k_{\text{max}} + 1)$  equations; and an infinite number of unknowns. However, the  $\gamma_{\ell m}(f)$  decay rapidly for large  $\ell$ , effectively reducing the number of unknowns. The root-mean-square amplitude of the  $\gamma_{\ell m}(f)$ 's,

$$\sigma_{\ell}(f) = \sqrt{C_{\ell}(f)}, \tag{39}$$

provides a good estimate of how each order in  $\ell$  contributes to the sum in (37). Here  $C_{\ell}(f)$  is the usual angular power spectrum:

$$C_{\ell}(f) = \frac{1}{2\ell + 1} \sum_{m = -\ell}^{\ell} |\gamma_{\ell m}(f)|^{2}.$$
(40)

‡ The equation count follows from  $-k_{\text{max}} \leq k \leq k_{\text{max}}$  and the freedom to alternately set  $q_R$  and  $q_I$  equal to zero.

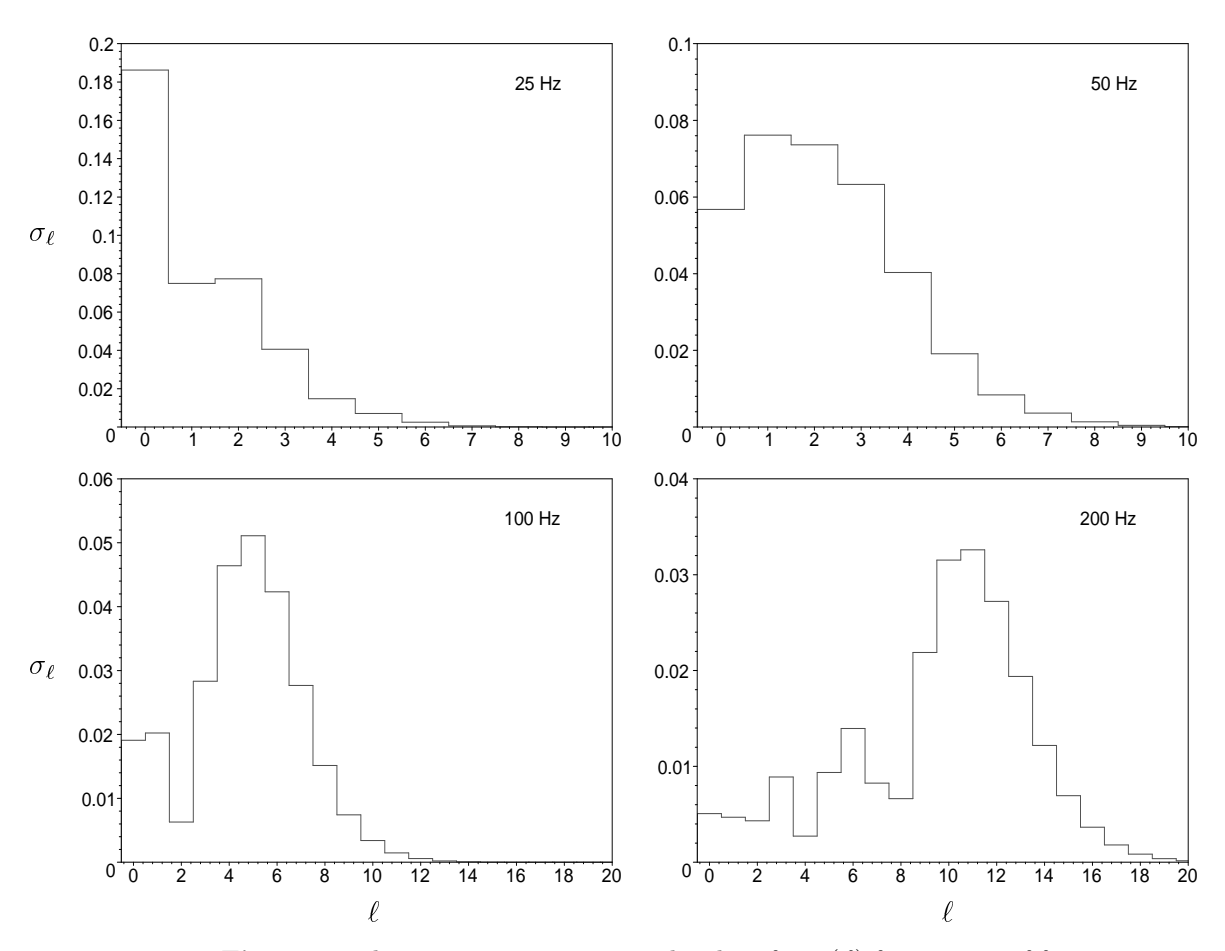


**Figure 2.** The root-mean-square amplitudes of  $\gamma_{\ell m}(f)$  for a range of frequencies.

Plots of  $\sigma_{\ell}(f)$  for f=25, 50, 100 and 200 Hz are shown in Figure 2. In each case, the low multipoles dominate the response. Thus, the sum (37) can be approximated by

$$C_k(f) = \sum_{\ell=|k|}^{\ell_{\text{max}}} p_{\ell k}(f) \, \gamma_{\ell k}(f) \,, \tag{41}$$

where  $\ell_{\text{max}} \approx 5$  for f = 25 Hz, rising to  $\ell_{\text{max}} \approx 18$  for f = 200 Hz. The number of equations is restricted to those with  $|k| \leq \ell_{\text{max}}$ . If we write  $C_k = q_R A_k + q_I B_k$  and use two sets of filters, one with  $q_R = 1$ ,  $q_I = 0$ , and the other with  $q_R = 0$  and  $q_I = 1$ , then (41) can be written as a set of  $4\ell_{\text{max}}$  equations for  $(\ell_{\text{max}} + 1)^2$  unknowns. As an example, consider the inversion problem at 25 Hz, where the system of equations is (for  $k \geq 0$ ):

$$A_{0} = p_{00}\gamma_{00} + p_{20}\gamma_{20} + p_{40}\gamma_{40} \qquad B_{0} = p_{10}\gamma_{10} + p_{30}\gamma_{30} + p_{50}\gamma_{50}$$

$$A_{1} = p_{21}\gamma_{21} + p_{41}\gamma_{41} \qquad B_{1} = p_{11}\gamma_{11} + p_{31}\gamma_{31} + p_{51}\gamma_{51}$$

$$A_{2} = p_{22}\gamma_{22} + p_{42}\gamma_{42} \qquad B_{2} = p_{32}\gamma_{32} + p_{52}\gamma_{52}$$

$$A_{3} = p_{43}\gamma_{43} \qquad B_{3} = p_{33}\gamma_{33} + p_{53}\gamma_{53}$$

$$A_{4} = p_{44}\gamma_{44} \qquad B_{4} = p_{54}\gamma_{54}$$

$$B_{5} = p_{55}\gamma_{55} . \qquad (42)$$

The above system of 20 equations involves 36  $p_{\ell m}$ 's, making it impossible to solve for each moment individually. The way around this impasse is to build another interferometer at a different location and to cross-correlate its output with the two LIGO detectors, in effect tripling the number of equations. Currently there are several interferometers being built in addition to the LIGO pair, including the Italian-French VIRGO detector near Pisa, the Anglo-German GEO detector near Hanover, and the Japanese TAMA detector near Tokyo. Cross-correlating the signals from all of these detectors will give roughly  $40\ell_{\rm max}$  equations for the  $(\ell_{\rm max}+1)^2$  unknowns, making it possible to create maps of the gravitational wave background with a resolution as high as  $\ell_{\rm max} \sim 38$ . Indeed, the limitation on the resolution will not come from the system being under determined, but from the lack of antenna sensitivity at high  $\ell$ .

## 4. Map making with LISA

The procedure for making a map of the gravitational wave sky with the LISA detector is very similar to the procedure we used for the LIGO detectors. Currently there are no plans to fly two sets of LISA spacecraft, so we will probably have to make do with the self-correlated signal from a single detector. At first sight it would appear that correlated noise in the self-correlated signal will prevent us from being able to distinguishing detector noise from a stochastic gravitational wave signal. However, this turns out not to be the case. Firstly, it is possible to discriminate between detector noise and a stochastic signal by using the Sagnac signal that is formed by comparing the phase of a signal that is sent clockwise around the LISA triangle with a signal that is sent counter-clockwise[11, 12]. The Sagnac signal is very insensitive to gravitational waves, making it the perfect tool for monitoring instrument noise. Secondly, the signal will vary periodically as the detector sweeps across the sky whereas the noise will not. Thus, by making several complete sweeps, it is possible to build up the signal to noise ratio in the measurements of  $C_k$  for all  $k \neq 0$ . We study the map making capabilities of a single LISA interferometer and a pair of optimally cross-correlated LISA interferometers. The optimal cross-correlation is achieved by placing six LISA spacecraft in a circle, with two sets of three spacecraft forming independent interferometers rotated by 90 degrees in the plane of the circle[13].

Proceeding as we did in the last section, the cross-correlated signal is given by

$$C(t,f) = \oint_{S^2} \mathcal{L}(\theta,\phi,f) \mathcal{F}(\theta,\phi,f,t) \sin \theta d\theta d\phi, \qquad (43)$$

where the luminosity is again given by

$$\mathcal{L}(\theta, \phi, f) = S_h(f)P(\widehat{\Omega}), \tag{44}$$

and the detector response function has the form

$$\mathcal{F}(\theta, \phi, f, t) = \frac{T\Delta f q_R}{4\pi} \Re \left[ \sum_{A=+,\times} F_1^A(\widehat{\Omega}, f, t) F_2^{A^*}(\widehat{\Omega}, f, t) e^{2\pi i f \widehat{\Omega} \cdot \Delta \mathbf{x}(t)/c} \right]$$

$$-\frac{T\Delta f q_I}{4\pi} \Im \left[ \sum_{A=+,\times} F_1^A(\widehat{\Omega}, f, t) F_2^{A*}(\widehat{\Omega}, f, t) e^{2\pi i f \widehat{\Omega} \cdot \Delta \mathbf{x}(t)/c} \right]. \tag{45}$$

While the basic expressions are similar for LISA and LIGO, the LISA antenna patterns are considerably more complicated:

$$F_i^A(\widehat{\Omega}, f, t) = \mathbf{D}_i(\widehat{\Omega}, f, t) : \mathbf{e}^A(\widehat{\Omega})$$
(46)

where

$$\mathbf{D}(\widehat{\Omega}, f, t) = \frac{1}{2} \left( (\mathbf{u}(t) \otimes \mathbf{u}(t)) \, \mathcal{T}(\mathbf{u} \cdot \widehat{\Omega}, f) - (\mathbf{v}(t) \otimes \mathbf{v}(t)) \, \mathcal{T}(\mathbf{v} \cdot \widehat{\Omega}, f) \right), \tag{47}$$

is the detector tensor and

$$\mathcal{T}(\mathbf{a} \cdot \widehat{\Omega}, f) = \frac{1}{2} \left[ \operatorname{sinc} \left( \frac{f}{2f_*} (1 - \mathbf{a} \cdot \widehat{\Omega}) \right) \exp \left( -i \frac{f}{2f_*} (3 + \mathbf{a} \cdot \widehat{\Omega}) \right) + \operatorname{sinc} \left( \frac{f}{2f_*} (1 + \mathbf{a} \cdot \widehat{\Omega}) \right) \exp \left( -i \frac{f}{2f_*} (1 + \mathbf{a} \cdot \widehat{\Omega}) \right) \right], \tag{48}$$

is the transfer function[14]. The transfer frequency,  $f_* = c/(2\pi L)$ , corresponds to a wave that just fits inside the interferometer. The LISA interferometer will have arms of length  $L = 5 \times 10^6$  km. The antenna pattern sweeps over the sky as the LISA constellation orbits about the Sun with period  $T_{\odot} = 1$  sidereal year. Setting  $k_{\text{max}} = 50$  fixes the integration period to be T = 315581 s (roughly three and a half days).

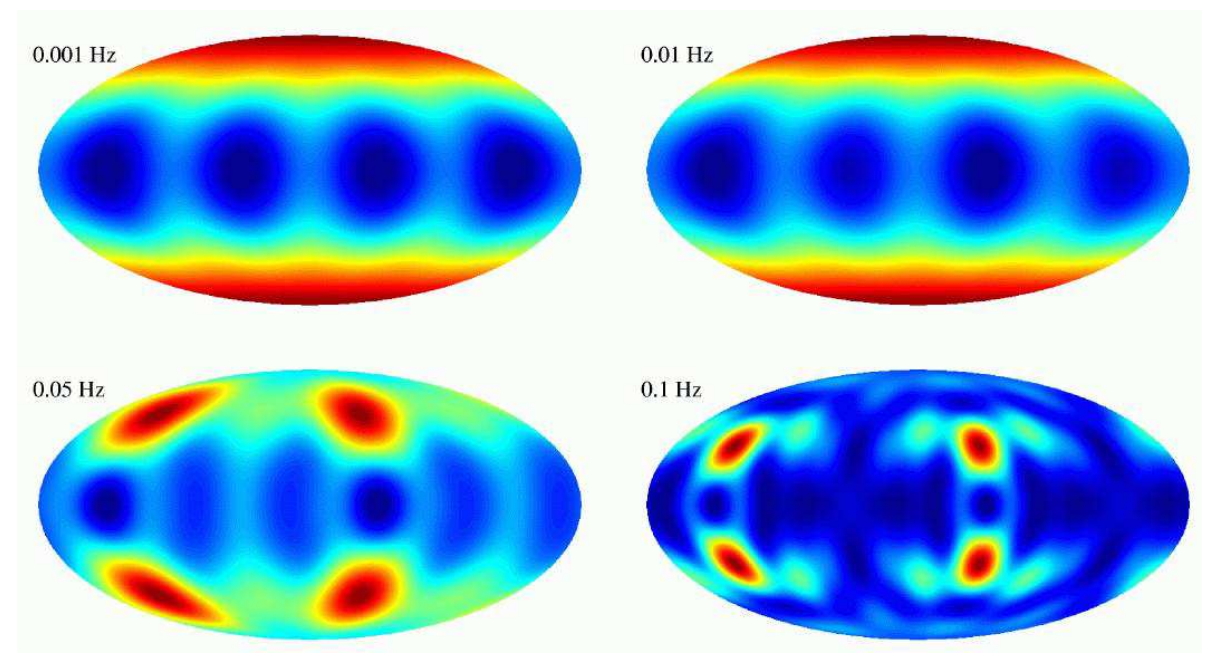


**Figure 3.** The antenna pattern for the self-correlated LISA detector in the detector rest frame for a range of frequencies.

Choosing Sky-fixed and LISA-fixed coordinate systems with their z axes normal to the ecliptic gives two frames of reference related by

$$\vec{e}_{\bar{x}} = \frac{1}{\sqrt{8}} (2 - \cos^2 \alpha - \cos \alpha \sin \alpha) \vec{e}_x + \frac{1}{\sqrt{8}} (1 + \cos^2 \alpha - \cos \alpha \sin \alpha) \vec{e}_y$$

$$-\frac{\sqrt{3}}{\sqrt{8}}(\cos\alpha + \sin\alpha)\vec{e}_z$$

$$\vec{e}_{\bar{y}} = \frac{1}{\sqrt{8}}(-2 + \cos^2\alpha - \cos\alpha\sin\alpha)\vec{e}_x + \frac{1}{\sqrt{8}}(1 + \cos^2\alpha + \cos\alpha\sin\alpha)\vec{e}_y$$

$$+\frac{\sqrt{3}}{\sqrt{8}}(\cos\alpha - \sin\alpha)\vec{e}_z$$

$$\vec{e}_{\bar{z}} = \frac{\sqrt{3}}{2}\cos\alpha\vec{e}_x + \frac{\sqrt{3}}{2}\sin\alpha\vec{e}_y + \frac{1}{2}\vec{e}_z,$$
(49)

where the bar denotes the LISA-fixed frame. The complicated scan pattern means that we have to calculate each rotation coefficient  $\lambda_{k\ell mn}$  individually. Since the coordinate transformation  $\Lambda_{ij}(\alpha)$  is second order in  $e^{i\alpha}$ , the index k will run from  $-2\ell$  to  $2\ell$ . To order  $\ell = 2$  the rotation coefficients are:

$$\lambda_{0000} = 1 \qquad \lambda_{01-1-1} = \frac{3\sqrt{2}}{8} \left(1+i\right) \qquad \lambda_{11-10} = \frac{\sqrt{6}}{4}$$

$$\lambda_{21-11} = \frac{\sqrt{2}}{8} \left(1-i\right) \qquad \lambda_{-110-1} = -\frac{\sqrt{3}}{4} \left(1+i\right) \qquad \lambda_{0100} = \frac{1}{2}$$

$$\lambda_{1101} = \frac{\sqrt{3}}{4} \left(1-i\right) \qquad \lambda_{-211-1} = \frac{\sqrt{2}}{8} \left(1+i\right) \qquad \lambda_{-1110} = -\frac{\sqrt{6}}{4}$$

$$\lambda_{0111} = \frac{3\sqrt{2}}{8} \left(1-i\right) \qquad \lambda_{02-2-2} = \frac{9i}{16} \qquad \lambda_{12-2-1} = \frac{3\sqrt{6}}{16} \left(1+i\right)$$

$$\lambda_{22-20} = \frac{3\sqrt{150}}{80} \qquad \lambda_{32-21} = \frac{\sqrt{6}}{16} \left(1-i\right) \qquad \lambda_{42-22} = -\frac{i}{16}$$

$$\lambda_{-12-1-2} = -\frac{3\sqrt{3}i}{8} \qquad \lambda_{12-10} = \frac{3\sqrt{2}}{8} \qquad \lambda_{22-11} = \frac{\sqrt{2}}{4} \left(1-i\right) \qquad (50)$$

$$\lambda_{32-12} = -\frac{\sqrt{3}i}{8} \qquad \lambda_{-220-2} = \frac{3\sqrt{150}i}{80} \qquad \lambda_{-120-1} = -\frac{3}{8} \left(1+i\right)$$

$$\lambda_{0200} = -\frac{1}{8} \qquad \lambda_{1201} = \frac{3}{8} \left(1-i\right) \qquad \lambda_{2202} = -\frac{3\sqrt{150}i}{80}$$

$$\lambda_{-321-2} = -\frac{\sqrt{3}i}{8} \qquad \lambda_{-221-1} = \frac{\sqrt{2}}{4} \left(1+i\right) \qquad \lambda_{-1210} = -\frac{3\sqrt{2}}{8}$$

$$\lambda_{1212} = -\frac{3\sqrt{3}i}{8} \qquad \lambda_{-422-2} = \frac{i}{16} \qquad \lambda_{-322-1} = -\frac{\sqrt{6}}{16} \left(1+i\right)$$

$$\lambda_{-2220} = \frac{3\sqrt{150}}{80} \qquad \lambda_{-1221} = -\frac{\sqrt{6}}{16} \left(1-i\right) \qquad \lambda_{0222} = -\frac{9i}{16}$$

Then antenna patterns for a self-correlated LISA detector and an optimally cross-correlated pair of LISA interferometers are shown in Figures 3, 4 and 5 for a range of frequencies in the rest frame of the detectors. These patterns can be turned into  $\bar{a}_{\ell m}$ 's using the HEALPIX software package[10]. In combination with the analytically derived rotation coefficients,  $\lambda_{k\ell mn}$ , the  $\bar{a}_{\ell m}$ 's yield the  $\gamma_{k\ell m}$ 's that appear in the deconvolution problem (15). In the low frequency limit,  $f \ll f_*$ , it is possible to derive the antenna harmonics  $\bar{a}_{\ell m}$  analytically. For the self-correlated LISA detector the non-vanishing

harmonics at zero frequency are:

$$\bar{a}_{00} = 1$$

$$\bar{a}_{20} = \frac{2\sqrt{5}}{7}$$

$$\bar{a}_{4-4} = \frac{\sqrt{70}}{84} + i\frac{\sqrt{210}}{252}$$

$$\bar{a}_{40} = \frac{1}{42}$$

$$\bar{a}_{44} = \frac{\sqrt{70}}{84} - i\frac{\sqrt{210}}{252}$$
(51)

while for the optimally cross-correlated pair of LISA detectors

$$\bar{a}_{00} = -1$$

$$\bar{a}_{20} = -\frac{2\sqrt{5}}{7}$$

$$\bar{a}_{4-4} = -\frac{\sqrt{70}}{84}$$

$$\bar{a}_{40} = -\frac{1}{42}$$

$$\bar{a}_{44} = -\frac{\sqrt{70}}{84}.$$
(52)

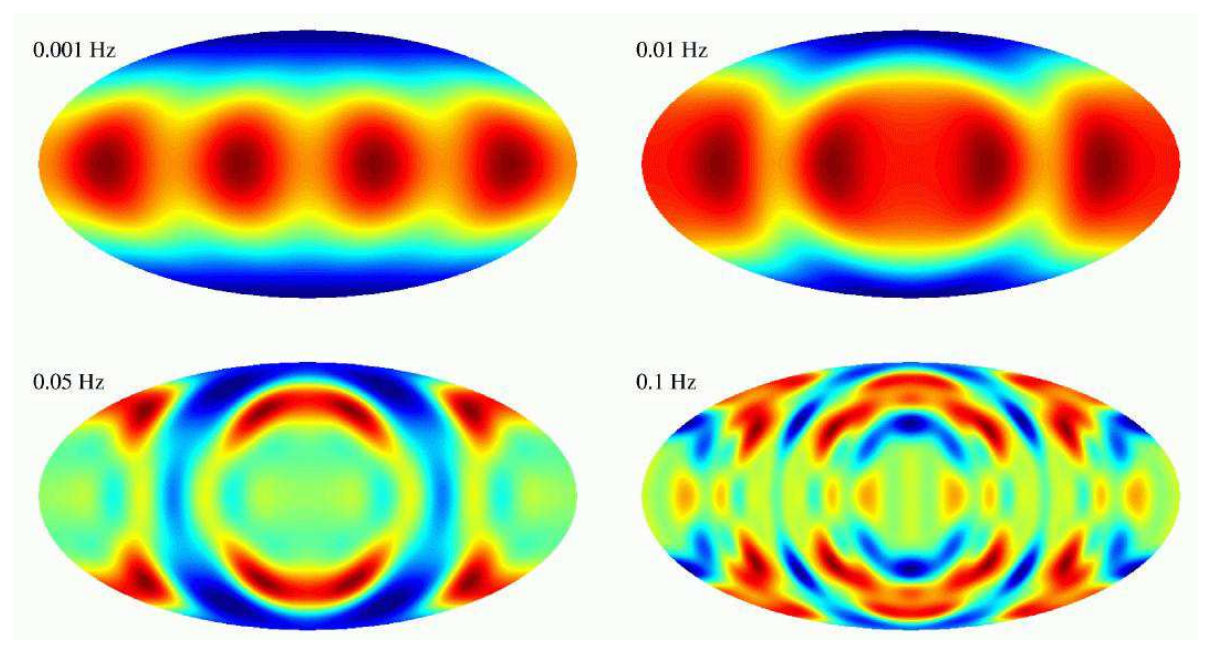


**Figure 4.** The antenna pattern for two optimally cross-correlated LISA detectors in the detector rest frame for a range of frequencies. Here  $q_R = 1$  and  $q_I = 0$ .

Combined with the rotation coefficients  $\lambda_{k\ell mn}$ , these give the  $\gamma_{k\ell m}$ 's that we need to solve the deconvolution problem in the low frequency limit. For example, the self-

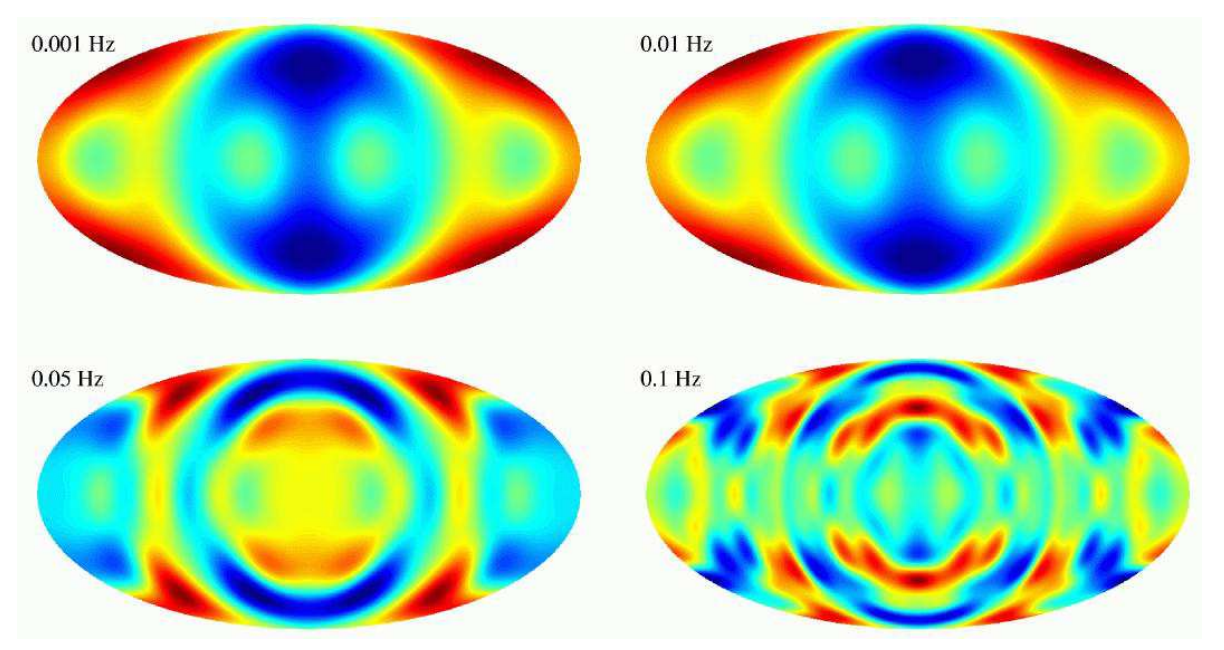


**Figure 5.** The antenna pattern for two optimally cross-correlated LISA detectors in the detector rest frame for a range of frequencies. Here  $q_R = 0$  and  $q_I = 1$ .

correlated LISA detector has

$$\gamma_{000} = 1 \qquad \gamma_{222} = \frac{3\sqrt{30}}{56} \qquad \gamma_{121} = -\frac{3\sqrt{10}}{28} \qquad \gamma_{020} = -\frac{\sqrt{5}}{28}$$

$$\gamma_{-12-1} = \frac{3\sqrt{10}}{28} \qquad \gamma_{-22-2} = \frac{3\sqrt{30}}{56} \qquad \gamma_{044} = -\frac{27\sqrt{70}}{7168} \qquad \gamma_{444} = \frac{3\sqrt{70}}{3584}$$

$$\gamma_{844} = -\frac{\sqrt{70}}{21504} \qquad \gamma_{-14-3} = -\frac{9\sqrt{105}}{1792} \qquad \gamma_{343} = -\frac{\sqrt{105}}{896} \qquad \gamma_{743} = \frac{\sqrt{105}}{5376}$$

$$\gamma_{-242} = \frac{9\sqrt{10}}{512} \qquad \gamma_{242} = \frac{3\sqrt{10}}{1792} \qquad \gamma_{642} = -\frac{\sqrt{10}}{512} \qquad \gamma_{-341} = -\frac{3\sqrt{15}}{256}$$

$$\gamma_{141} = \frac{5\sqrt{15}}{2688} \qquad \gamma_{541} = \frac{\sqrt{15}}{256} \qquad \gamma_{-440} = -\frac{15}{512} \qquad \gamma_{040} = -\frac{37}{5376} \qquad (53)$$

$$\gamma_{440} = -\frac{15}{512} \qquad \gamma_{-54-1} = -\frac{\sqrt{15}}{256} \qquad \gamma_{-14-1} = -\frac{5\sqrt{15}}{2688} \qquad \gamma_{34-1} = \frac{3\sqrt{15}}{256}$$

$$\gamma_{-64-2} = -\frac{\sqrt{10}}{512} \qquad \gamma_{-24-2} = \frac{3\sqrt{10}}{1792} \qquad \gamma_{24-2} = -\frac{9\sqrt{10}}{512} \qquad \gamma_{-74-3} = -\frac{\sqrt{105}}{5376}$$

$$\gamma_{-34-3} = \frac{\sqrt{105}}{896} \qquad \gamma_{14-3} = \frac{9\sqrt{105}}{1792} \qquad \gamma_{-84-4} = -\frac{\sqrt{70}}{21504} \qquad \gamma_{-44-4} = \frac{3\sqrt{70}}{3584}$$

$$\gamma_{04-4} = -\frac{27\sqrt{70}}{7168} \qquad .$$

Thus, at very low frequencies, the inversion problem only involves  $|k| \leq 8$  and multipoles with  $\ell=0,2$  and 4, which gives us 17 equations for 15 unknowns. Writing out the convolution problem explicitly reveals that the system is simultaneously under and over constrained. In other words, some individual multipoles will be very well determined while others can only be given in combination with other multipoles. Once again the degeneracy can be split by building additional detectors that make different antenna sweeps. Alternatively, the LISA constellation could be re-position after several years of data collection into a new orbit that is inclined with respect to the ecliptic.

At higher frequencies the LISA detectors are sensitive to more multipoles. Plots of the root-mean-square amplitude,  $\sigma_{\ell}(f)$ , of the antenna multipoles  $\bar{a}_{\ell m}$  are shown in

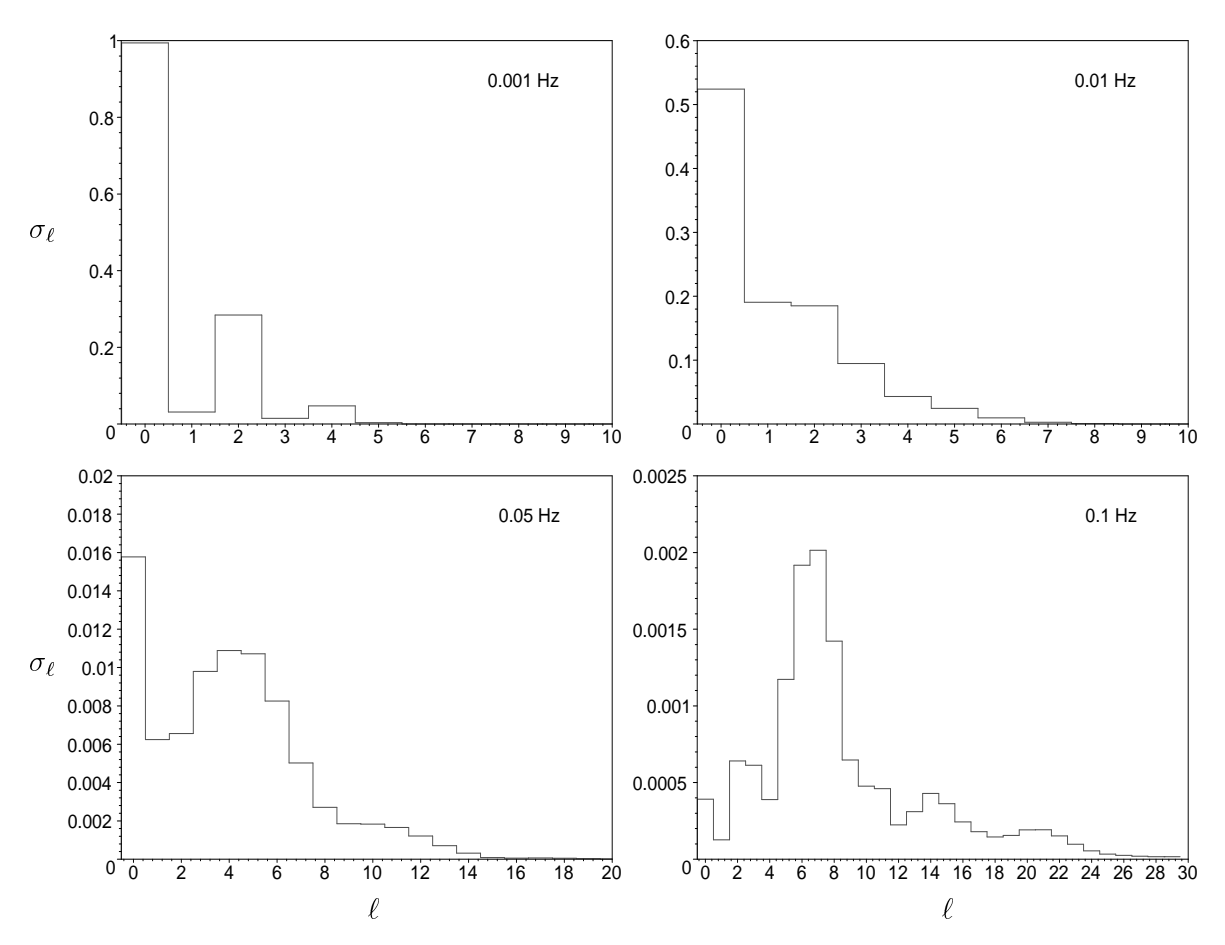


**Figure 6.** The root-mean-square amplitudes of  $\bar{a}_{\ell m}(f)$  for the optimally cross-correlated LISA detectors at a range of frequencies.

Figure 6 for the optimally cross-correlated LISA detectors. By either re-positioning the LISA constellation or by flying multiple constellations at different inclinations, it will be possible to produce maps with a resolution approaching  $\ell=25$ , which corresponds to an angular resolution of seven degrees.

## Acknowledgments

I benefitted from discussion with Shane Larson, Ron Hellings and Bill Hiscock. I would like to thank Kris Gorski for help with the *HEALPIX* software package.

### References

- [1] Abramovici A et al. 1992 Science 256 325.
- [2] Bender P L et al. 1998 LISA Pre-Phase A Report.
- [3] Jaranowski P & Królak A 1999 Phys. Rev. D**59** 063003.
- [4] Peterseim M, Jennrich O, Danzmann K & Schutz B F, 1996 Class. Quantum Grav. 14, 1507.
- [5] Cutler C, 1998 Phys. Rev. D57, 7089.
- [6] Hellings R W & Moore T A, 2000 Phys. Rev. D to appear.

- [7] Allen A & Ottewill A C, 1997 Phys. Rev. D56, 545.
- [8] Giampieri G & Polnorev A G, 1997 Mon. Not. Roy. Astrn. Soc. 291, 149.
- [9] Cornish N J & Larson S L 2001, in preparation.
- [10] Gorski K M, Wandelt B D, Hivon E, Hansen F K & Banday A J, http://www.eso.org/kgorski/healpix/.
- [11] Tinto M, Armstrong J W & Estabrook F B 2001 Phys. Rev. D63, 021101(R).
- [12] Hogan C J & Bender P L, 2001 astro-ph/0104266.
- [13] Cornish N J 2001, in preparation.
- [14] Cornish N J & Larson S L 2001, Class. Quantum Grav. to appear (gr-qc/0103075).